Physics Letters A 383 (2019) 759–763

Contents lists available at ScienceDirect

Physics Letters A

www.elsevier.com/locate/pla

While rotating while cloaking

Liliang Zhou [a], Shiyao Huang [a], Meng Wang [b], Run Hu [a,*], Xiaobing Luo [a]

[a] School of Energy and Power Engineering, Huazhong University of Science and Technology, Wuhan 430074, China
[b] China–EU Institute for Clean and Renewable Energy, Huazhong University of Science and Technology, Wuhan 430074, China

ARTICLE INFO

Article history:
Received 20 September 2018
Received in revised form 16 November 2018
Accepted 26 November 2018
Available online 28 November 2018
Communicated by R. Wu

Keywords:
Transformation thermotics
Coordinate transformation
Thermal cloak
Thermal rotator

ABSTRACT

Invisible optical and thermal cloaking have been explored as the typical demonstrations of the transformation optics and thermotics theory. However, the existing cloaks are realized by only one-coordinate transformation, and the cloaking layout, i.e. the form of electromagnetic wave/heat passing around the invisible region, is single for a long time. Here, we propose a new rotated thermal cloak which can unify the conventional cloaking and rotating together, and realize the while-rotating–while-cloaking effect. The required anisotropic thermal conductivity tensor is deduced from the new geometric mapping. Though rotated, the heat flux can be tuned around the central invisible region perfectly by the proposed rotated thermal cloak. The underlying physics is explored by comprehensive analysis of the distribution of the thermal conductivity tensor, which is further compared with those of the conventional cloak and rotator. The experimental feasibility is also discussed by validating the practical while-rotating–while-cloaking effect through a proof-of-concept design. The proposed rotated thermal cloak is expected to extend the possibility of cloaking scheme, and open avenues for the multiple coordinate transformation in counterpart physical fields, like optics, electrics, acoustics, magnetics, mechanics, etc.

© 2018 Elsevier B.V. All rights reserved.

1. Introduction

Since the birth of transformation optics (TO), the invisible cloak has attracted lots of interests due to its *ad hoc* characteristic that can render any object inside invisible to the electromagnetic (EM) radiation [1]. In other word, people cannot see the object inside from certain direction, which has been extensively described in fictions or popular movies over centuries. The essence of TO lies the invariance of the Maxwell equation under the coordinate transformation from the virtual space to the real space, but resulting in the undesired, anisotropic, inhomogeneous permittivity and permeability in the cloaking layer in return. Though difficult, experimental physicists have realized such optical invisible cloak by different methods [2,3]. Many people have devoted to the extension of TO theory and the invisible cloak to other physical fields, such as acoustics [4], thermotics [5–11], mechanics [12], or even quantum mechanics [13]. Similar to TO, the heat conduction equation is proven to be form-invariant under coordinate transformation, and the counterpart transformation thermotics and thermal cloak are proposed. As for thermal cloak, the heat flux can be tuned around the invisible region and return to their original direction, without disturbing the heat flux and isotherms outside at all, which looks as if there was no object inside. Due to the lacking of phase information, thermal cloak tends to be more attractive and likely to be achieved for heat flux manipulation than the EM counterparts. For instance, the heat flux has been manipulated to realize thermal cloaking [14–18], concentrating [19,20], rotating [21], refracting [22], reflecting [23], and camouflaging [7,24,25], encoding [26] with successful validation in theory or in experiments.

As far as we are concerned, the optical or thermal cloak is realized almost by the same geometric transformation, $\{r' = \frac{b-a}{b}r + a, \theta' = \theta, z' = z'\}$, where a and b are the inner and outer radii of the annular cloaking structure. By such geometric transformation, we can easily map a cylinder with radius of b in the virtual space into an annular structure with radii of a and b in the real space. As a result, the cylinder with radius of a in the real space corresponds to a singularity in the virtual space and forms the invisible region. Such a mapping relationship is simple, effective and successful, but only transforms one coordinate (like r) while maintaining other coordinates (like θ and z) invariant. Can we deduce other kinds of geometric mapping for advanced optical or thermal cloaking effect? To answer this question, we propose a new kind of geometric mapping in this study and validate the transformation effect in thermal field.

* Corresponding author.
E-mail address: hurun@hust.edu.cn (R. Hu).

https://doi.org/10.1016/j.physleta.2018.11.041
0375-9601/© 2018 Elsevier B.V. All rights reserved.

2. Transformation thermotics

To deduce the transformed properties for cloaking metamaterials, we have to introduce the transformation thermotics in brief. Heat conduction without heat source is governed by Fourier's law as $\rho c\frac{\partial T}{\partial t}=\nabla\cdot(\boldsymbol{\kappa}\nabla T)$, where ρ and c are the density and thermal capacity, $\boldsymbol{\kappa}$ is the thermal conductivity tensor, and T is the temperature. According to the principle of the transformation thermotics, the Fourier equation maintains the form after coordinate transformation, i.e. $\rho' c'\frac{\partial T'}{\partial t}=\nabla'\cdot(\boldsymbol{\kappa}'\nabla T')$. The transformed thermal conductivity tensor from the virtual space (x, y, z) to the real space (x', y', z'), which can be expressed as [5,7]

$$\boldsymbol{\kappa}'=\begin{bmatrix}\kappa'_{xx}&\kappa'_{xy}&\kappa'_{xz}\\ \kappa'_{yx}&\kappa'_{yy}&\kappa'_{yz}\\ \kappa'_{zx}&\kappa'_{zy}&\kappa'_{zz}\end{bmatrix}=\frac{\mathbf{J}\kappa_0\mathbf{J}^{\mathrm{T}}}{\det(\mathbf{J})} \tag{1}$$

with

$$\begin{aligned}\mathbf{J}&=\frac{\partial(x',y',z')}{\partial(x,y,z)}=\mathbf{J}_{x'r'}\mathbf{J}_{r'r}\mathbf{J}_{rx}\\ &=\frac{\partial(x',y',z')}{\partial(r',\theta',z')}\frac{\partial(r',\theta',z')}{\partial(r,\theta,z)}\frac{\partial(r,\theta,z)}{\partial(x,y,z)}\end{aligned} \tag{2}$$

where κ_0 is the homogeneous thermal conductivity in the virtual space, $\mathbf{J}$ is the Jacobian matrix of the two spaces and $\mathbf{J}^{\mathrm{T}}$ is the transposition of $\mathbf{J}$. To realize the advanced thermal cloaking effect, following geometric mapping is used

$$\begin{cases}r'=\dfrac{b-a}{b}r+a,\\ \theta'=\theta+\theta_0\dfrac{b-r}{b-a},\\ z'=z.\end{cases} \tag{3}$$

By such mapping, the virtual space is not only compressed into an annular region, but also rotated by a predesigned angle from θ_0 to 0 gradually with the increase of r. Here, two coordinates are transformed, which is different from the conventional one. Substituting Eq. (3) into Eq. (2) and neglecting the z coordinate for simplification, we first obtain

$$\begin{aligned}\mathbf{J}&=\begin{bmatrix}\frac{\partial x'}{\partial r'}&\frac{\partial x'}{\partial\theta'}\\ \frac{\partial y'}{\partial r'}&\frac{\partial y'}{\partial\theta'}\end{bmatrix}\begin{bmatrix}\frac{b-a}{b}&0\\ \frac{-\theta_0}{b-a}&1\end{bmatrix}\begin{bmatrix}\frac{\partial r}{\partial x}&\frac{\partial r}{\partial y}\\ \frac{\partial\theta}{\partial x}&\frac{\partial\theta}{\partial y}\end{bmatrix}\\ &=\mathbf{R}(\theta')diag(1,r')\begin{bmatrix}\frac{b-a}{b}&0\\ \frac{-\theta_0}{b-a}&1\end{bmatrix}diag\left(1,\frac{1}{r}\right)\mathbf{R}(\theta)^{\mathrm{T}}\end{aligned} \tag{4}$$

where $\mathbf{R}(\theta')$ and $\mathbf{R}(\theta)$ are the rotational matrixes of the real space and the virtual space with $\mathbf{R}(\varphi)=\begin{bmatrix}\cos\varphi&-\sin\varphi\\ \sin\varphi&\cos\varphi\end{bmatrix}$. By substituting Eq. (4) into Eq. (1) with $\mathbf{R}(\theta)^{\mathrm{T}}=\mathbf{R}(\theta)^{-1}$, we can obtain the transformed thermal conductivity tensor as

$$\begin{aligned}\boldsymbol{\kappa}'&=\mathbf{R}(\theta')\begin{bmatrix}\kappa'_{11}&\kappa'_{12}\\ \kappa'_{21}&\kappa'_{22}\end{bmatrix}\mathbf{R}(\theta')^{-1}\kappa_0\\ &=\mathbf{R}(\theta')\begin{bmatrix}\frac{r'-a}{r'}&\frac{-b\theta_0(r'-a)}{(b-a)^2}\\ \frac{-b\theta_0(r'-a)}{(b-a)^2}&\frac{r'}{r'-a}+\frac{b^2\theta_0^2r'(r'-a)}{(b-a)^4}\end{bmatrix}\mathbf{R}(\theta')^{-1}\kappa_0.\end{aligned} \tag{5}$$

It is seen in Eq. (5) that the required $\boldsymbol{\kappa}'$ is more anisotropic with off-diagonal components. With such transformed thermal conductivity, we can validate our idea with finite element simulations.

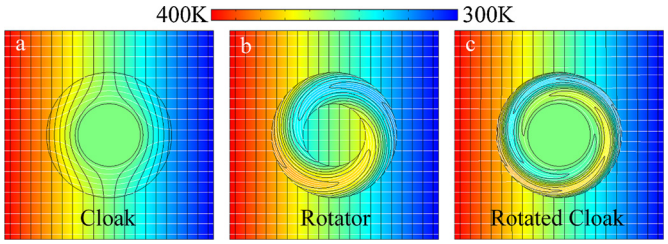

Fig. 1. Temperature profile comparisons among conventional cloak, rotator and the proposed rotated cloak. The black grid lines denote the isotherms and the white lines denotes heat flux lines. Left and right boundaries are kept at 400 K and 300 K, respectively. The reference homogeneous material for the whole plane except for the annular cloaking structure is polydimethylsiloxane (PDMS) with $\kappa_0=0.16$ W(m · K), $\rho=970$ kg/m^3, and $c=1460$ J/(kg · K). The thermal properties of the annular cloaking structure are according to the calculation. The radius of the annular region is 15 mm and 30 mm. The dimension of the whole plane is 100 mm × 100 mm. (For interpretation of the colors in the figures, the reader is referred to the web version of this article.)

3. Results and discussions

Firstly, we would like to vividly show the differences of the thermal functionalities among conventional cloak, rotator and the proposed rotated cloak. Heat is conducted from the left boundary to the right without convection, and the steady temperature fields are shown in Fig. 1 through the commercial software COMSOL (http://www.comsol.com). In all the cases, the heat flux lines are parallel to the x-direction and the isotherms are perpendicular to the x-direction outside the annular region, which look like as if heat conducts along a homogenous plane without the annular region. In the annular region, the heat flux lines are tuned gradually without passing through the central invisible region in Fig. 1(a). This is the conventional outside thermal camouflage by the invisible thermal cloak. Fig. 1(b) shows the steady temperature profile of the conventional thermal rotator [18,27]. It is seen that the heat flux lines are rotated by $\theta_0=\pi$ and the heat flux is inverted in the central region. The proposed rotated cloak is shown in Fig. 1(c). Comparing Figs. 1(c) and 1(b), we can see that the main difference is in the central region: in the proposed rotated thermal cloak, the heat flux lines and isotherms don't enter the central region; while in the conventional thermal rotator, the heat flux lines and isotherms enter the central region. The proposed structure can realize two functions, i.e. thermal cloaking and thermal rotating, thus it is called as rotated thermal cloak hereinafter.

The simulated steady temperature profiles with different predesigned rotation angles are shown in Fig. 2. In the annular region, the heat flux lines and the isotherms are rotated in an anti-clockwise direction gradually with the increase of predesign rotation angle θ_0. The larger the θ_0 is, the stronger the temperature profiles are rotated. More importantly, though the temperature profiles in the annular region are rotated, they never pass through the central region. The heat flux lines are tuned around the central region and return to their original direction before entering the annular region, which is the basic requirement of thermal cloaking. From Eq. (5), when the predesign rotation angle θ_0 vanishes, the required $\boldsymbol{\kappa}'$ can be simplified as $\boldsymbol{\kappa}'=\mathbf{R}(\theta')diag(\frac{r'-a}{r'},\frac{r'}{r'-a})\mathbf{R}(\theta')^{-1}\kappa_0$, which is exactly the same as that of the conventional thermal cloak, and the corresponding temperature field is shown in Fig. 1(a). Another difference is that the temperature profiles in the proposed rotated thermal cloak are rotated stronger than that in the conventional thermal rotator though the predesign rotation angle θ_0 in both cases are the same as $\theta_0=\pi$.

To explain the reason, we plot the variation of each component of the transformed $\boldsymbol{\kappa}'$ at different locations with comparisons among the conventional cloak, rotator, and the proposed rotated

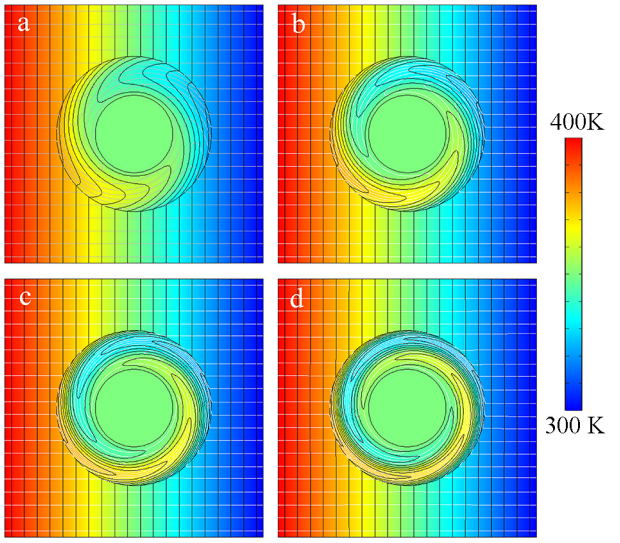

Fig. 2. Snapshots of steady temperature profiles of rotated thermal cloaks with different predesigned rotation angles: (a) $\theta_0 = \pi/4$, (b) $\theta_0 = \pi/2$, (c) $\theta_0 = 3\pi/4$ and (d) $\theta_0 = \pi$. All the boundary conditions maintain the same with Fig. 1.

cloak, as shown in Fig. 3. According to the transformation thermotics, the transformed thermal conductivity tensors in the cylindrical coordinate for the conventional thermal cloak and concentrator are

$$\boldsymbol{\kappa}'_{\text{cloak}} = \begin{bmatrix} \frac{r'-a}{r'} & 0 \\ 0 & \frac{r'}{r'-a} \end{bmatrix} \kappa_0, \tag{6}$$

and

$$\boldsymbol{\kappa}'_{\text{rotator}} = \begin{bmatrix} 1 & -\frac{r'\theta_0}{b-a} \\ -\frac{r'\theta_0}{b-a} & 1+\frac{\theta_0^2 r'^2}{(b-a)^2} \end{bmatrix} \kappa_0. \tag{7}$$

Comparing Eqs. (5)–(7), we may find that the radial components κ'_{11} of the cloak and the rotated cloak are the same, which are independent of rotation angle θ_0 and increases with the increase of r', therefore the curves overlap in Fig. 3(a). The off-diagonal components κ'_{12} and κ'_{21} are the same for the cloak, concentrator and the rotated cloak. For the conventional cloak, κ'_{12} is identical with 0. For the rotator and the rotated cloak, κ'_{12} are linear functions of r' and proportional to θ_0. When r' or θ_0 increases in Fig. 3(b), the value of κ'_{12} decreases monotonously but magnitude increases due to negative sign in the formula. We also can see that for certain θ_0, the magnitude of κ'_{12} of the rotated cloak is always larger than that of the rotator. For the tangential component κ'_{22}, it is non-monotonous as shown in Fig. 3(c). When r' increases from the inner boundary to the outer boundary of the annular cloaking region, κ'_{22} decreases monotonously for the conventional

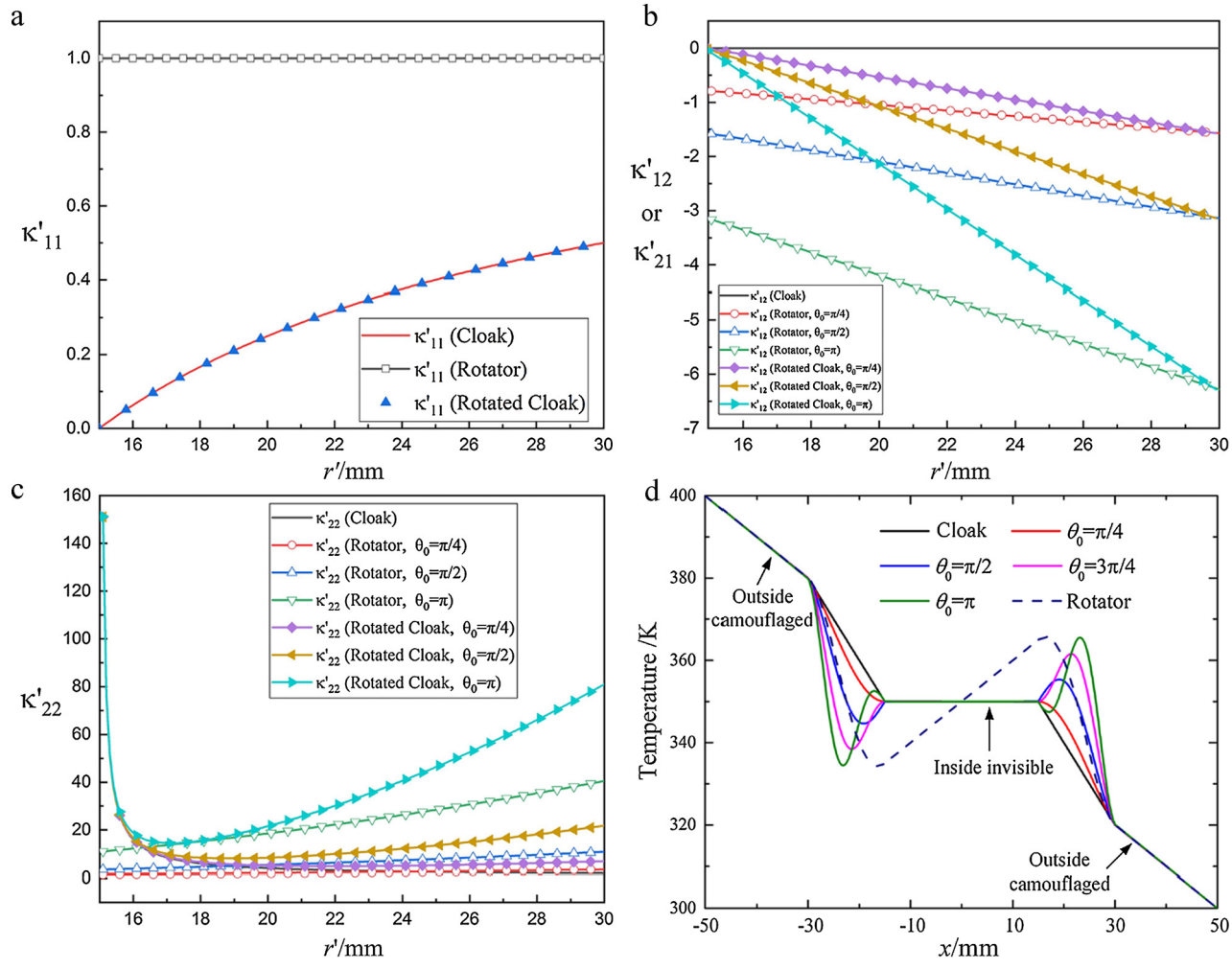

Fig. 3. Comparison of each component of the transformed thermal conductivity tensors among conventional cloak, rotator and rotated cloak with r' and θ_0: (a) κ'_{11}, (b) κ'_{12} and κ'_{21}, (c) κ'_{22}. (d) Temperature distribution of central lines along x-direction in Figs. 1 and 2.

cloak, increases monotonously for the conventional rotator, while decreases rapidly first and then increases gradually for the rotated cloak. The influence of θ_0 seems negligible until r' becomes larger than ~17 mm. Larger θ_0 leads to larger tangential component at large r'. Compared to the magnitude of κ'_{22}, the other components of $\boldsymbol{\kappa}'$ are much smaller but significant for the realization of rotated thermal cloaking effect. In particular, when r' approaches the inner boundary at $r' = a$, there exists a singularity and κ'_{22} tends to be infinite, which implies an infinite value of tangential thermal conductivity there and a constant temperature at the ring of $r' = a$. Also, we can find that for certain θ_0, the magnitude of κ'_{22} of the rotated cloak is always larger than that of the rotator, corresponding to the stronger rotation in Fig. 1(c) than the conventional rotator in Fig. 1(b).

To clearly observe the thermal cloaking effect, we plot the temperature distribution of the central lines along x-direction of each subfigure of Figs. 1 and 2. It is seen in Fig. 3(d) that along the x-direction (the direction of heat conducts), the temperature decreases for all cases. In the outside region, the temperature curves overlap with each other, implying the outside camouflage for the proposed rotated thermal cloak. In the annular cloaking region, the temperature curves change with the rotation angle θ_0. Larger θ_0 leads to larger temperature slops and stronger temperature changes. With the approaching of the inner boundary, the temperature drops rapidly first and then increases to the same level of the inside central region. In the inside central region, all the temperature curves overlap with each other again at constant temperature of 350 K, i.e. the average temperature of the two boundaries. The constant temperature in the central region implies the inside invisibility, which is the expected outcome of thermal cloak. We also plot the temperature curve of the conventional cloak and rotator in Figs. 1(a) and 1(c) in Fig. 3(d). The main difference is in the central region. There is a reverse temperature gradient in the central region with that in the outside, which looks as if heat conducts from the right to the left and gives rise to the concept of apparent negative thermal conductivity (ANTC) [5,6]. Re-checking the annular region, we may see that there also exists ANTC in the annular region and there tends to have multiple inflection points (peaks and valleys) in the temperature curves. It is also seen that the temperature slop of the conventional rotator with $\theta_0 = \pi$ is equivalent to the proposed rotated thermal cloak with $\theta_0 = \pi/2$, which corresponds to the stronger rotation effect in Fig. 1(c) than in Fig. 1(b). The negative value of the off-diagonal component of the transformed thermal conductivity tensor $\boldsymbol{\kappa}'$ can be solved such as effective medium theory (EMT) [7,8], and here, according to the formula of the negative component, i.e. $\kappa'_{12} = \frac{-b\theta_0(r'-a)}{(b-a)^2}$, we can easily assign the rotation angle from θ_0 to $-\theta_0$, and the negative sign can be eliminated. A simple demonstration can be seen from Figs. 4(a) and 4(b), where we only change the rotation angle from $\theta_0 = +\pi$ to $\theta_0 = -\pi$ and maintain all the other simulation conditions. We can successfully see the rotated thermal cloaking effect in both two subfigures and the only difference is the rotation direction: one is anti-clockwise and the other is clockwise. To experimentally fabricate such rotated cloak, we can take advantage of the existing fabrication strategies of the conventional cloak and rotator. For the fabrication of the conventional cloak, we can use concentric rings of two kinds of materials of relatively large difference in thermal conductivity, like copper and PDMS [15,19]. Heat tends to be conducted along the copper rings without entering the central region, achieving the thermal cloaking effect. For the fabrication of the conventional rotator, we can use the alternative rotated-layers of two materials, like copper and PDMS [21,27]. Heat can be conducted along the rotated copper layers, achieving the thermal rotating effect. Inspired by such strategies, we can design a structure composed by concentric layers and rotated layers, as shown in Fig. 4(c). In our proof-of-concept design, we use 3 concentric copper layers and 8 rotated copper layers, and the remaining region is filled with PDMS. In our simulation, the boundary conditions are kept the same with previous FEM simulations, and the simulated temperature field is shown in Fig. 4(d). It is seen that heat is rotated in the annular region without entering the central region, thus achieving the while-rotating–while-cloaking effect.

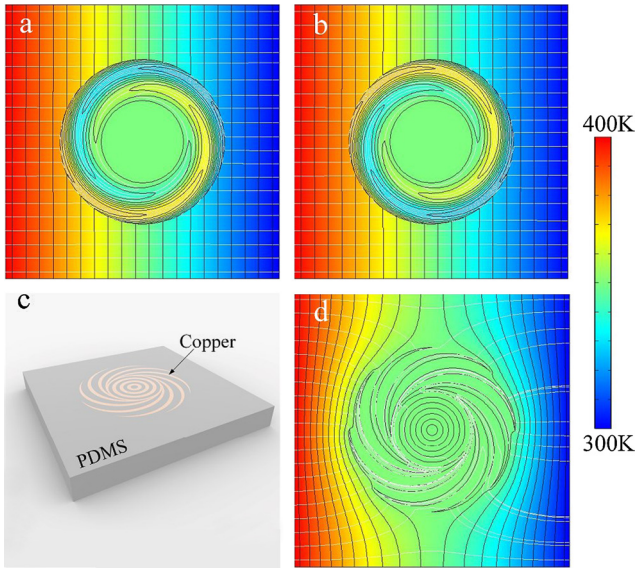

Fig. 4. Snapshots of steady temperature profiles of the rotated thermal cloak with (a) $\theta_0 = +\pi$ and (b) $\theta_0 = -\pi$. (c) Schematic of the experimental design scheme for the rotated cloak, which is composed by concentric copper/PDMS rings and rotated copper/PDMS layers. (d) Simulated temperature field of the experimental design. All the boundary conditions maintain the same with Fig. 1.

4. Conclusions

In summary, we proposed a new rotated thermal cloak which can unify the conventional thermal cloaking and rotating functionalities and realize the while-rotating–while-cloaking effect. The required anisotropic thermal conductivity tensor is deduced from the new geometric mapping and the simulation processes are introduced. Through finite element simulation validation, the proposed rotated thermal cloak is proven to realize the conventional thermal cloaking at zero rotation angle, and to realize rotated thermal cloaking at non-zero rotation angle, which is the extension of conventional thermal cloak. Though rotated, the heat flux can be tuned around the central invisible region perfectly by the proposed rotated thermal cloak. The underlying physics is explored by comprehensive analysis of the distribution of the thermal conductivity tensor, with comparison among those of the conventional cloak and rotator. For practical fabrication, a proof-of-concept design is also presented, which is composed by concentric copper/PDMS rings and rotated copper/PDMS layers simultaneously. The proposed rotated thermal cloak is expected to extend the possibility of cloaking scheme, and open avenues for the similar multiple coordinate transformation simultaneously in all counterpart physical fields, such as electromagnetic, optics, acoustics, electrics, mechanics, etc.

Acknowledgements

The authors would like to acknowledge the financial support from the National Natural Science Foundation of China (Grant Nos. 51606074 and 51625601), the Ministry of Science and Technology of the People's Republic of China (Project No. 2017YFE0100600), and the National Key Research and Development Program of China (Project No. 2016YFB0400804).

References

[1] J.B. Pendry, D. Shurig, D.R. Smith, Science 312 (2006) 1780.
[2] T.C. Han, C.W. Qiu, X.H. Tang, Opt. Lett. 35 (2010) 2642–2644.
[3] B. Kanté, D. Germain, A. de Lustrac, Phys. Rev. B 80 (2009) 201104(R).
[4] L. Zigoneanu, B.I. Popa, S.A. Cummer, Nat. Mater. 13 (2014) 352.
[5] C.Z. Fan, Y. Gao, J.P. Huang, Appl. Phys. Lett. 92 (2008) 251907.
[6] S. Guenneau, C. Amra, D. Veynante, Opt. Express 20 (7) (2012) 8207.
[7] R. Hu, S.L. Zhou, Y. Li, D.Y. Lei, X.B. Luo, C.W. Qiu, Adv. Mater. 30 (2018) 1707237.
[8] S.L. Zhou, R. Hu, X.B. Luo, Int. J. Heat Mass Transf. 127 (2018) 114–121.
[9] X.Y. Shen, Y. Li, C.R. Jiang, J.P. Huang, Phys. Rev. Lett. 117 (2016) 055501.
[10] Y. Li, X.Y. Shen, Z.H. Wu, J.Y. Huang, Y.X. Chen, Y.S. Ni, J.P. Huang, Phys. Rev. Lett. 115 (2015) 195503.
[11] Y. Li, X.Y. Shen, J.P. Huang, Y.S. Ni, Phys. Lett. A 380 (2016) 1641–1647.
[12] T. Bückmann, M. Thiel, M. Kadic, R. Schittny, M. Wegener, Nat. Commun. 5 (2014) 4130.
[13] S. Zhang, D.A. Genov, C. Sun, X. Zhang, Phys. Rev. Lett. 100 (2008) 123002.
[14] D.M. Nguyen, H. Xu, Y. Zhang, B.L. Zhang, Appl. Phys. Lett. 107 (2015) 121901.
[15] T. Han, X. Bai, D. Gao, J.T.L. Thong, B.W. Li, C.W. Qiu, Phys. Rev. Lett. 112 (2014) 054302.
[16] R. Hu, S.L. Zhou, X.J. Yu, X.B. Luo, J. Phys. D, Appl. Phys. 49 (2016) 415302.
[17] R. Hu, J. Hu, R. Wu, B. Xie, X. Yu, X.B. Luo, Chin. Phys. Lett. 33 (4) (2016) 044401.
[18] E.M. Dede, T. Nomura, P. Schmalenberg, J.S. Lee, Appl. Phys. Lett. 103 (2013) 063501.
[19] R. Hu, X.L. Wei, J.Y. Hu, X.B. Luo, Sci. Rep. 4 (2014) 3600.
[20] F. Chen, D.Y. Lei, Sci. Rep. 5 (2015) 11552.
[21] S. Guenneau, C. Amra, Opt. Express 21 (5) (2013) 6578.
[22] R. Hu, B. Xie, J.Y. Hu, Q. Chen, X.B. Luo, Europhys. Lett. 111 (2015) 54003.
[23] R. Hu, S.L. Zhou, W.C. Shu, B. Xie, Y.P. Ma, X.B. Luo, AIP Adv. 6 (2016) 125111.
[24] T.C. Han, X. Bai, J.T.L. Thong, B.W. Li, C.W. Qiu, Adv. Mater. 26 (2014) 1731–1734.
[25] X. He, L.Z. Wu, Appl. Phys. Lett. 105 (2014) 221904.
[26] R. Hu, S.Y. Huang, M. Wang, L.L. Zhou, X.Y. Peng, X.B. Luo, Phys. Rev. Appl. 10 (2018) 054032.
[27] H. Chen, C.T. Chan, Appl. Phys. Lett. 90 (2007) 241105.